View metadata, citation and similar papers at core.ac.uk
brought to you by CORE
provided by Infoscience - École polytechnique fédérale de Lausanne

A Robust Data-Driven Controller Design Methodology With Applications to Particle Accelerator Power Converters

Achille Nicoletti, Michele Martino, and Alireza Karimi

***Abstract*— A new data-driven approach using the frequency response function (FRF) of a system is proposed for designing robust-fixed structure digital controllers for particle accelerators' power converters. This design method ensures that the dynamics of a system are captured and avoid the problem of unmodeled dynamics associated with parametric models. The H_∞ robust performance condition can be represented by a set of convex constraints with respect to the parameters of a two degree of freedom RST controller. This controller is robust with respect to the frequency-dependent uncertainties of the FRF. A convex optimization algorithm is implemented to obtain the controller parameters. The effectiveness of the method is illustrated by considering two case studies that require robust controllers for achieving the desired performance.**

***Index Terms*— Convex optimization, data-driven control, H-infinity, power converter control, robust control, RST.**

I. Introduction

MANY of today's complex systems possess a multitude of uncertainties, and obtaining an accurate parametric model for such systems can be both laborious and impractical for controller synthesis. In industrial schemes, the dynamics of plants are typically approximated by low-order models, since the controller synthesis is easier to implement for lower order processes. However, this approximation can impede the performance of a controller, since low-order models are subject to model uncertainty. A survey on the differences associated with model-based control and data-driven control has been addressed in [1] and [2]; Hou and wang [1] and Bazanella [2] assert that the model-based control methods are inherently less robust due to the unmodeled dynamics of a process, and that these controllers are unsafe for practical applications. With the data-driven control scheme, the parametric uncertainties and the unmodeled dynamics (for linear time-invariant systems) are irrelevant and the only source of uncertainty comes from the measurement process.

Data-driven control methods using frequency-domain data are design schemes that continue to spark the interest of many researchers. Hoogendijk *et al.* [3] use the frequency response data of a stable system to design an optimal controller through a symmetric root locus technique. A robust frequency-domain control design method has been established in [4]; this method, however, requires a solution to a nonlinear optimization problem. A frequency-domain loop-shaping approach to design fixed-structure controllers is presented in [5]. In this method, a convex optimization problem can be formulated if a linearly parameterized controller is considered; however, in this method, the closed-loop stability is not guaranteed and should be verified *a posteriori*.

Robust controller design methods belonging to the $\mathcal{H}_\infty$ control framework minimize the $\mathcal{H}_\infty$ norm of a weighted closed-loop sensitivity function. In [6], a frequency-response method is proposed based on the Q-parametrization to guarantee the $\mathcal{H}_\infty$ performance for fixed-structure controllers. In [7], a frequency-domain approach is realized where a convex optimization algorithm is formulated by considering a convex approximation of the $\mathcal{H}_\infty$ criterion (using linearly parameterized controllers). This method is extended to data-driven gain-scheduled controller design in [8] and multivariable decoupling controller design in [9]. A frequency-domain approach for computing linearly parameterized controllers are presented in [10] and [11], where the $\mathcal{H}_\infty$ constraints are convexified around an initial stabilizing controller; an iterative algorithm is used that converges to a local optimal solution of the nonconvex problem. The extension of this method to design multivariable proportional-integral-derivative controllers for stable systems is presented in [12]. The design of controllers that are not linear in parameters (i.e., represented by rational transfer functions) using frequency-domain data are studied in [13]. The necessary and sufficient conditions for the existence of such controllers are developed. This method needs no initial stabilizing controller and converges to the global solution of the $\mathcal{H}_\infty$ problem as the order of the controller increases.

The method proposed in this brief is an extension of [14], where the necessary and sufficient conditions that ensures the $\mathcal{H}_\infty$ performance for multiple weighted sensitivity functions are presented. In addition, since the parameters of the controller's denominator are the optimization variables, this method can lead to unstable controllers. Therefore, a sufficient condition is presented to ensure that the controller remains stable. In [14], a controller design was implemented that only considered the nominal model of the process; in this brief, the frequency-dependent uncertainties originating from the measurement process are taken into consideration for robust performance specifications. Moreover, it is shown that as the controller order increases, the solution to the $\mathcal{H}_\infty$ problem converges to the global solution (for the RST controller

Manuscript received October 5, 2017; accepted November 30, 2017. Date of publication February 8, 2018; date of current version February 8, 2019. Manuscript received in final form December 11, 2017. Recommended by Associate Editor P. F. F. Odgaard. *(Corresponding author: Achille Nicoletti.)*

A. Nicoletti is with the Technology Department, European Organization for Nuclear Research, CH-1211 Geneve, Switzerland, and also with the Automatic Control Laboratory, Ecole Polytechnique Fédérale de Lausanne, CH-1015 Lausanne, Switzerland (e-mail: achille.nicoletti@cern.ch).

M. Martino is with the Technology Department, European Organization for Nuclear Research, CH-1211 Geneve, Switzerland.

A. Karimi is with the Automatic Control Laboratory, Ecole Polytechnique Fédérale de Lausanne, CH-1015 Lausanne, Switzerland.

Color versions of one or more of the figures in this brief are available online at http://ieeexplore.ieee.org.

Digital Object Identifier 10.1109/TCST.2017.2783346

1063-6536 © 2018 IEEE. Personal use is permitted, but republication/redistribution requires IEEE permission.
See http://www.ieee.org/publications_standards/publications/rights/index.html for more information.

structure that considers multiple weighted sensitivity functions). The proposed method is used to design robust controllers for two case studies; in the first one, an unstable system with multimodel uncertainty is considered to illustrate the generality of the method, while in the second case (which constitutes the main applicative focus of this brief), a robust RST controller is designed for power converters in particle accelerators at the European Organization for Nuclear Research (CERN). The designed controller is implemented in the power converters to control their output current with extremely high precision, which represent its major challenge. The main advantage of the proposed data-driven method for this application is to simultaneously guarantee the robustness margins, attain the required bandwidth, and ensure a small tracking error while avoiding the long and tedious manual tuning process intrinsically involved in the classical pole-placement model-based approach.

The brief is organized as follows. The class of models, controllers, and control objectives are defined in Section II. Section III discusses the control design methodology and stability conditions of the proposed method for the RST controller structure. Convex conditions are formulated based on the $\mathcal{H}_\infty$ criterion. Section IV is dedicated to several case studies where the effectiveness of the method is demonstrated in both simulation and experiment. Finally, the concluding remarks are given in Section V.

II. Preliminaries

A. Class of Models

Let $u[k]$ and $y[k]$ represent the input and output signals of a causal discrete-time system, respectively, where k is a discrete-time instant and T_s is the sampling period. Suppose that these signals are noise free and have zero initial and final conditions (i.e., $u[k] = y[k] = 0$ for $k \leq 0$ and $k > K_s$). Then, the frequency response function (FRF) of the system can be represented as $G(e^{-j\omega}) = Y(e^{-j\omega})U^{-1}(e^{-j\omega})$, where

$$U(e^{-j\omega}) = \frac{1}{\sqrt{K_s}} \sum_{k=0}^{K_s} u[k] e^{-j\omega T_s k} \tag{1}$$

$$Y(e^{-j\omega}) = \frac{1}{\sqrt{K_s}} \sum_{k=0}^{K_s} y[k] e^{-j\omega T_s k} \tag{2}$$

are the periodograms of the input and output signals and $\omega \in [-\pi/T_s, \pi/T_s]$. Note that due to the symmetry of the periodograms, it is sufficient to consider $\omega \in [0, \pi/T_s]$ for practical applications. Under these assumptions, it is evident that from a set of sampled time-domain data, one is able to obtain a continuous FRF. If the data is noisy, then $G(e^{-j\omega})$ is characterized as the empirical transfer function estimate and is asymptotically unbiased [15]. For such systems, an additive uncertainty model can be considered to ensure robustness in the presence of noise perturbations.

Let the set $\mathscr{P}$ represents the family of all stable, proper, and real-rational transfer functions. It is imperative to note that $\mathscr{P}$ is closed under multiplication and addition; in other words,

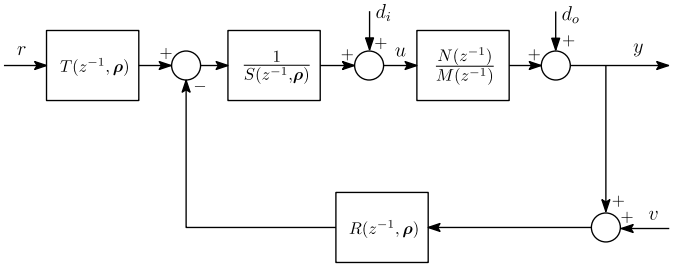

Fig. 1. RST controller structure.

if $P_1(z^{-1}), P_2(z^{-1}) \in \mathscr{P}$, then

$$\{P_1(z^{-1}) + P_2(z^{-1}),\, P_1(z^{-1})P_2(z^{-1})\} \in \mathscr{P} \tag{3}$$

where z is the complex frequency variable used to represent discrete-time systems. Suppose that a single-input-single-output feedback control system structure is used where the plant is represented as $G(z^{-1}) = N(z^{-1})M^{-1}(z^{-1})$ such that $\{N(z^{-1}), M(z^{-1})\} \in \mathscr{P}$ (where $N(z^{-1})$ and $M(z^{-1})$ are coprime factorizations over $\mathscr{P}$ [16]). Let the FRF of the plant be defined as $G(e^{-j\omega}) = N(e^{-j\omega})M^{-1}(e^{-j\omega})$ for all $\omega \in \Omega$, where $\Omega := [0, \pi/T_s]$. $N(e^{-j\omega})$ and $M(e^{-j\omega})$ must be FRFs of bounded analytic functions outside the unit circle; for a stable plant, a trivial choice is $N(e^{-j\omega}) = G(e^{-j\omega})$ and $M(e^{-j\omega}) = 1$. For unstable systems, a stabilizing controller is needed in order to properly formulate $N(e^{-j\omega})$ and $M(e^{-j\omega})$. In this case, $N(e^{-j\omega})$ is the FRF between the reference signal and the measured output, while $M(e^{-j\omega})$ is the FRF between the reference signal and the plant input. In general, a set $\mathcal{G}$ can be formulated to represent a plant model containing p FRF models: $\mathcal{G} = \{G_l(e^{-j\omega}); l = 1, \ldots, p; \forall\omega \in \Omega\}$. These FRFs can be determined by considering the frequency response of a parametric model or from a set of input-output data. For example, a pseudorandom binary sequence (PRBS) signal can be used as an excitation signal to identify the dynamics of a plant, since this type of signal has properties similar to white noise and excites all frequencies. Sine-sweep methods can also be used for this identification. For simplicity, one model from the set $\mathcal{G}$ will be considered, and the subscript l will be omitted. However, in general, the design procedures outlined in this brief can be applied to the multimodel case.

It is supposed that the uncertainty associated with a given FRF is described by an additive uncertainty of coprime factors

$$\begin{aligned} \hat{N}(e^{-j\omega}) &= N(e^{-j\omega}) + |W_n(e^{-j\omega})|\delta_n e^{j\theta_n} \\ \hat{M}(e^{-j\omega}) &= M(e^{-j\omega}) + |W_m(e^{-j\omega})|\delta_m e^{j\theta_m} \end{aligned} \tag{4}$$

where $|\delta_n| \leq 1$, $|\delta_m| \leq 1$; $\{\theta_n, \theta_m\} \in [0, 2\pi]$; and W_n and W_m are the uncertainty weighting filters which can be determined from the covariance of the estimates for a given confidence interval [15].

B. Class of Controllers

The controller structure that will be considered will be of the RST-type. The RST controller is a two degree of freedom controller which can be used to synthesize the tracking and

regulation requirements independently of each other [17]. The general structure of this controller is shown in Fig. 1. Each controller is realized as a polynomial function as follows:

$$R(z^{-1},\boldsymbol{\rho}) = r_0 + r_1 z^{-1} + \cdots + r_{n_r} z^{-n_r} \tag{5}$$

$$S(z^{-1},\boldsymbol{\rho}) = 1 + s_1 z^{-1} + \cdots + s_{n_s} z^{-n_s} \tag{6}$$

$$T(z^{-1},\boldsymbol{\rho}) = t_0 + t_1 z^{-1} + \cdots + t_{n_t} z^{-n_t} \tag{7}$$

where $\{n_r, n_s, n_t\}$ are the orders of the polynomials R, S, and T, respectively. The controller parameter vector $\boldsymbol{\rho} \in \mathbb{R}^{n_c}$ (vector of decision variables) is defined as

$$\boldsymbol{\rho}^\top = [r_0, r_1, \ldots, r_{n_r}, s_1, s_2, \ldots, s_{n_s}, t_0, t_1, \ldots, t_{n_t}]$$

where $n_c = n_r + n_s + n_t + 2$.

C. Sensitivity Functions

Since the design techniques introduced in this brief belong to the $\mathcal{H}_\infty$ framework, it is appropriate to consider the various sensitivity functions associated with the RST controller structure. Some sensitivity functions for this process can be asserted as follows:

$$\mathcal{S}_1(z^{-1},\boldsymbol{\rho}) = \frac{y}{d_o} = \frac{M(z^{-1})S(z^{-1},\boldsymbol{\rho})}{\psi(z^{-1},\boldsymbol{\rho})} \tag{8}$$

$$\mathcal{S}_2(z^{-1},\boldsymbol{\rho}) = \frac{y}{r} = \frac{N(z^{-1})T(z^{-1},\boldsymbol{\rho})}{\psi(z^{-1},\boldsymbol{\rho})} \tag{9}$$

$$\mathcal{S}_3(z^{-1},\boldsymbol{\rho}) = \frac{r-y}{r} = \frac{\psi(z^{-1},\boldsymbol{\rho}) - N(z^{-1})T(z^{-1},\boldsymbol{\rho})}{\psi(z^{-1},\boldsymbol{\rho})} \tag{10}$$

where $\psi(z^{-1},\boldsymbol{\rho}) = N(z^{-1})R(z^{-1},\boldsymbol{\rho}) + M(z^{-1})S(z^{-1},\boldsymbol{\rho})$, y is the system output, r is the reference input, and d_o is the output disturbance. For notation purposes, the dependence in z^{-1} will be omitted, and will only be reiterated when deemed necessary. Note that all of the sensitivity functions are stable if the zeros of $\psi(\boldsymbol{\rho})$ lie within the unit circle. The sensitivity functions defined above (and all other sensitivity functions of interest) all contain the same transfer function $\psi(\boldsymbol{\rho})$. Therefore, a general construction of the sensitivity function can be expressed as $\mathcal{S}_q(\boldsymbol{\rho}) = \Delta_q(\boldsymbol{\rho})/\psi(\boldsymbol{\rho})$, where $\Delta_q(\boldsymbol{\rho})$ is a linear function of R, S, and/or T. The subscript $q \in \{1, 2, \ldots, c\}$ denotes the q-th sensitivity of interest and c is the total number of sensitivity functions.

III. $\mathcal{H}_\infty$ Performance via Convex Optimization

A. General Design Specifications

In the general $\mathcal{H}_\infty$ control problem, the objective is to find the controller parameter vector $\boldsymbol{\rho}$ such that

$$\sup_{\omega\in\Omega} |H_q(e^{-j\omega},\boldsymbol{\rho})| < \gamma \tag{11}$$

where $\gamma \in \mathbb{R}_+$, $H_q(e^{-j\omega},\boldsymbol{\rho}) = W_q(e^{-j\omega})\mathcal{S}_q(e^{-j\omega},\boldsymbol{\rho})$, and W_q is the FRF of a stable weighting filter such that $H_q(e^{-j\omega},\boldsymbol{\rho})$ has a bounded infinity norm. For notation purposes, the dependence in $e^{-j\omega}$ will be omitted, and will only be reiterated when deemed necessary. The condition in (11) can also be expressed as follows:

$$\gamma^{-1}|W_q\Delta_q(\boldsymbol{\rho})| < |\psi(\boldsymbol{\rho})|; \quad \forall\omega\in\Omega. \tag{12}$$

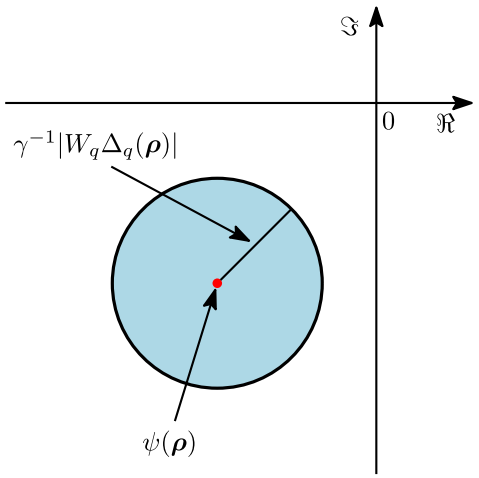

Fig. 2. Graphical interpretation of $\mathcal{H}_\infty$ constraints in the complex plane.

It is desired to minimize the upper bound γ such that the $\mathcal{H}_\infty$ performance condition is satisfied. Therefore, the following optimization problem can be considered:

$$\begin{aligned} &\min_{\gamma,\boldsymbol{\rho}} \gamma \\ &\text{s.t.: } \gamma^{-1}|W_q\Delta_q(\boldsymbol{\rho})| < |\psi(\boldsymbol{\rho})| \\ &\qquad \forall\omega\in\Omega; \quad q\in\mathcal{Q}\subset\{1,2,\ldots,c\}. \end{aligned} \tag{13}$$

Notice that (13) is a nonconvex optimization problem.

Consider a circle in the complex plane at a specific frequency in Ω which is centered at $\psi(\boldsymbol{\rho})$ and has radius $\gamma^{-1}|W_q\Delta_q(\boldsymbol{\rho})|$. The constraint in (12) ensures that for any frequency point in Ω, the circle associated with this frequency point will not encircle the origin. Fig. 2 displays the graphical interpretation of this condition. This geometrical construction will be used to prove the following Lemma.

Lemma 1: Suppose that

$$H_q(e^{-j\omega},\boldsymbol{\rho}) = W_q(e^{-j\omega})\Delta_q(e^{-j\omega},\boldsymbol{\rho})\psi^{-1}(e^{-j\omega},\boldsymbol{\rho})$$

is the frequency response of a bounded analytic function outside the unit circle. Then, the following constraint is met:

$$\sup_{\omega\in\Omega} |H_q(e^{-j\omega},\boldsymbol{\rho})| < \gamma \tag{14}$$

if and only if there exists a stable function $F(z^{-1})$ that satisfies

$$\Re\{\psi(\boldsymbol{\rho})F(e^{-j\omega})\} > \gamma^{-1}|W_q\Delta_q(\boldsymbol{\rho})F(e^{-j\omega})|, \quad \forall\omega\in\Omega.$$

Proof: The basic idea is similar to that of the proof of [18, Th. 1]. It is clear that (14) is satisfied if and only if the disk of radius $\gamma^{-1}|W_q\Delta_q(\boldsymbol{\rho})|$ centered at $\psi(\boldsymbol{\rho})$ does not include the origin for all $\omega\in\Omega$, i.e., $|\psi(\boldsymbol{\rho})| > \gamma^{-1}|W_q\Delta_q(\boldsymbol{\rho})|$. This is equivalent to the existence of a line passing through the origin that does not intersect the disk. Therefore, at every given frequency ω, there exists a complex number $f(e^{-j\omega})$ that can rotate the disk such that it lays inside the right-hand side of the imaginary axis. Hence, we have

$$\begin{aligned} &\Re\{[\psi(\boldsymbol{\rho}) - \gamma^{-1}|W_q\Delta_q(\boldsymbol{\rho})|e^{j\theta}]f(e^{-j\omega})\} > 0 \\ &\qquad\qquad \forall\omega\in\Omega, \quad \forall\theta\in[0,\ 2\pi] \end{aligned} \tag{15}$$

where $\Re\{\cdot\}$ denotes the real part of the argument. Since $f(e^{-j\omega}) = |f(e^{-j\omega})|e^{j\theta_f}$, then (15) can be expressed as

$$\Re\{\psi(\boldsymbol{\rho})f(e^{-j\omega})\} > \gamma^{-1}|W_q\Delta_q(\boldsymbol{\rho})f(e^{-j\omega})|\cos(\theta+\theta_f) \quad \forall\omega\in\Omega,\quad \forall\theta\in[0,\ 2\pi]. \tag{16}$$

However, (16) is satisfied if and only if

$$\Re\{\psi(\boldsymbol{\rho})f(e^{-j\omega})\} > \gamma^{-1}|W_q\Delta_q(\boldsymbol{\rho})f(e^{-j\omega})| \quad \forall\omega\in\Omega. \tag{17}$$

In [18], it is shown that, $f(e^{-j\omega})$ can be approximated arbitrarily well by the frequency response of a stable transfer function or FIR function $F(z^{-1})$ if and only if

$$Z = \left(\psi(\boldsymbol{\rho}) - \gamma_0^{-1}|W_q\Delta_q(\boldsymbol{\rho})|e^{j\theta}\right)^{-1} \tag{18}$$

is analytic outside the unit circle for all $\gamma_0 > \gamma$ and all $\theta \in [0,\ 2\pi]$. However, $\psi^{-1}(\boldsymbol{\rho})$ is stable because of the stability of $H_q(\boldsymbol{\rho})$. On the other hand, by decreasing γ_0 from infinity to γ, the poles of Z move continuously with γ_0. Therefore, Z is not analytic outside the unit circle (i.e., Z has poles outside the unit circle) if and only if $Z^{-1}(e^{-j\omega}) = 0$ for a given frequency, which is not the case because the origin is not in the interior of the circle $\gamma_0^{-1}|W_q\Delta_q(\boldsymbol{\rho})|e^{j\theta}$. ■

The set of all controllers that meet the performance condition defined by the weighted norm of sensitivity functions is asserted in the following theorem.

Theorem 1: Given the FRF $G(e^{-j\omega}) = N(e^{-j\omega})M^{-1}(e^{-j\omega})$ and the frequency response of a weighting filter $W_q(e^{-j\omega})$, then the following statements are equivalent for a given $q \in \mathcal{Q}$.

1) There exists an RST controller that stabilizes G and

$$\sup_{\omega\in\Omega}|W_q\mathcal{S}_q(\boldsymbol{\rho})| < \gamma. \tag{19}$$

2) There exists an RST controller such that

$$\Re\{\psi(\boldsymbol{\rho})\} > \gamma^{-1}|W_q\Delta_q(\boldsymbol{\rho})| \quad \forall\omega\in\Omega. \tag{20}$$

*Proof (**b** $\Rightarrow$ **a**):* $\psi(\boldsymbol{\rho})$ is analytic outside the unit circle and its real part is positive for all $\omega \in \Omega$. Therefore, $\psi(\boldsymbol{\rho})$ will not encircle the origin when ω travels along the Nyquist contour, and its inverse is stable. This implies that $R(\boldsymbol{\rho})$ and $S(\boldsymbol{\rho})$ stabilizes G. On the other hand, we have

$$|\psi(\boldsymbol{\rho})| \geq \Re\{\psi(\boldsymbol{\rho})\} \quad \forall\omega\in\Omega$$

which leads to $|W_q\Delta_q(\boldsymbol{\rho})| < \gamma|\psi(\boldsymbol{\rho})|$ for all $\omega \in \Omega$ and to (19) in Statement (**a**).

*(**a** $\Rightarrow$ **b**):* Assume that $R(\boldsymbol{\rho}_0)$, $S(\boldsymbol{\rho}_0)$, and/or $T(\boldsymbol{\rho}_0)$ satisfy Statement (**a**) but not Statement (**b**). Then, according to Lemma 1, there exists a FIR function $F(z^{-1})$ such that

$$\Re\{\psi(\boldsymbol{\rho}_0)F(e^{-j\omega})\} > \gamma^{-1}|W_q\Delta_q(\boldsymbol{\rho}_0)F(e^{-j\omega})| \tag{21}$$

for all $\omega \in \Omega$. Therefore, there exists a higher order RST controller with $R = R(\boldsymbol{\rho}_0)F$, $S = S(\boldsymbol{\rho}_0)F$, and/or $T = T(\boldsymbol{\rho}_0)F$ such that Statement (**b**) holds. ■

The above theorem gives a necessary and sufficient condition for satisfying the $\mathcal{H}_\infty$ criterion for *one* sensitivity function. However, in typical control system applications, it is desired to shape several sensitivity functions simultaneously and impose multiple constraints on the weighted sensitivity functions. The following theorem ensures necessity and sufficiency of the $\mathcal{H}_\infty$ criterion when multiple sensitivity functions are considered.

Theorem 2: Given the FRF $G(e^{-j\omega}) = N(e^{-j\omega})M^{-1}(e^{-j\omega})$ and the frequency response of weighting filters $W_q(e^{-j\omega})$ for $\forall q \in \mathcal{Q}$, then the following statements are equivalent.

1) There exists an RST controller that stabilizes G and

$$\sup_{\omega\in\Omega}|W_q\mathcal{S}_q(\boldsymbol{\rho})| < \gamma \quad \forall q\in\mathcal{Q}. \tag{22}$$

2) There exists an RST controller such that

$$\Re\{\psi(\boldsymbol{\rho})\} > \gamma^{-1}|W_q\Delta_q(\boldsymbol{\rho})| \quad \forall\omega\in\Omega \tag{23}$$

and for all $q \in \mathcal{Q}$.

*Proof (**b** $\Rightarrow$ **a**):* The proof for this condition is equivalent to the proof presented in Theorem 1. By satisfying the constraint in (23) for all $q \in \mathcal{Q}$, the condition in (22) for each corresponding q is obtained.

*(**a** $\Rightarrow$ **b**):* Assume that $R(\boldsymbol{\rho}_0)$, $S(\boldsymbol{\rho}_0)$, and/or $T(\boldsymbol{\rho}_0)$ satisfy Statement (**a**) but not Statement (**b**). Then, according to Lemma 1, there exist FIR transfer functions $F_q(z^{-1})$ such that

$$\Re\{F_q\psi(\boldsymbol{\rho}_0) - \gamma^{-1}|F_qW_q\Delta_q(\boldsymbol{\rho}_0)|\} > 0 \tag{24}$$

for all $\omega \in \Omega$ and for all $q \in \mathcal{Q}$. For Statement (**b**) to hold, there must exist a common F for all $q \in \mathcal{Q}$ such that $R = R(\boldsymbol{\rho}_0)F$, $S = S(\boldsymbol{\rho}_0)F$, and/or $T = T(\boldsymbol{\rho}_0)F$.

For a given frequency, the constraints in (22) will represent circles in the complex plane that are centered exactly at $\psi(\boldsymbol{\rho}_0)$ with varying radii (where the radii depend on each q). Let us define the following quantities at every $\omega \in \Omega$:

$$\begin{aligned}\Pi(e^{-j\omega},\boldsymbol{\rho}_0) &:= \{|W_1\Delta_1(e^{-j\omega},\boldsymbol{\rho}_0)|,\ldots,|W_c\Delta_c(e^{-j\omega},\boldsymbol{\rho}_0)|\}\\ r_\pi(e^{-j\omega},\boldsymbol{\rho}_0) &:= \gamma^{-1}\max_{q\in\mathcal{Q}}\Pi(e^{-j\omega},\boldsymbol{\rho}_0).\end{aligned} \tag{25}$$

For any ω, the circle with radius $r_\pi(\boldsymbol{\rho}_0)$ does not include the origin, and all of the other circles with smaller radii are enclosed in the circle with radius $r_\pi(\boldsymbol{\rho}_0)$, that is

$$\gamma^{-1}|W_q\Delta_q(e^{-j\omega},\boldsymbol{\rho}_0)| \leq r_\pi(e^{-j\omega},\boldsymbol{\rho}_0).$$

Therefore, for a given frequency, the complex number f_q which is used to rotate the circle associated with radius $r_\pi(e^{-j\omega},\boldsymbol{\rho}_0)$ ensures that all of the circles with $\gamma^{-1}|W_q\Delta_q(e^{-j\omega},\boldsymbol{\rho}_0)| \leq r_\pi(e^{-j\omega},\boldsymbol{\rho}_0)$ are also rotated such that they all lie in the right-hand side of the imaginary axis. Therefore, there will always exist a common F that interpolates all f_q (different q in different frequencies) such that the conditions in (24) hold true for all $q \in \mathcal{Q}$. ■

B. Robust Design

With the proposed method, it is possible to design a fixed-structure controller which accounts for the uncertainties of a given FRF (as described in Section II-A). Given this additive uncertainty, a desired performance condition $\|W_q\mathcal{S}_q\|_\infty < \gamma$ will be satisfied for all models in the uncertain set (4) if $\|W_q\hat{\mathcal{S}}_q\|_\infty < \gamma$, where $\hat{\mathcal{S}}_q = \hat{\Delta}_q/\hat{\psi}(\boldsymbol{\rho})$ and $\hat{\psi}(\boldsymbol{\rho}) = \hat{N}R(\boldsymbol{\rho}) + \hat{M}S(\boldsymbol{\rho})$. For example, consider the nominal performance condition $\|W_3\hat{\mathcal{S}}_3\|_\infty < \gamma$ with $\hat{\Delta}_3(\boldsymbol{\rho}) = \hat{M}S(\boldsymbol{\rho}) + \hat{N}[R(\boldsymbol{\rho}) - T(\boldsymbol{\rho})]$; as a worst case consideration, δ_m and δ_n can

be selected to be equal to one in (4) (which ensures that the uncertainty in the entire disk is taken into account). By substituting the expressions in (4) into this condition, the following constraint can be devised:

$$|W_3[\psi(\boldsymbol{\rho}) - NT(\boldsymbol{\rho}) + S(\boldsymbol{\rho})|W_m|e^{j\theta_m} + C(\boldsymbol{\rho})|W_n|e^{j\theta_n}]| < \gamma\,|\psi(\boldsymbol{\rho}) + R(\boldsymbol{\rho})|W_n|e^{j\theta_n} + S(\boldsymbol{\rho})|W_m|e^{j\theta_m}| \quad (26)$$

$\forall\omega \in \Omega, \forall\{\theta_n, \theta_m\} \in [0, 2\pi]$, where $C(\boldsymbol{\rho}) = R(\boldsymbol{\rho}) - T(\boldsymbol{\rho})$. For notation purposes, let $\psi'(\boldsymbol{\rho}, \theta_n) := \psi(\boldsymbol{\rho}) + R(\boldsymbol{\rho})|W_n|e^{j\theta_n}$ be defined. Then for a given $\{\omega, \theta_n, \theta_m\}$, (26) represents a circle centered at $\psi'(\boldsymbol{\rho}, \theta_n) + S(\boldsymbol{\rho})|W_m|e^{j\theta_m}$ with a radius of

$$x_p(\boldsymbol{\rho}, \theta_m, \theta_n) = \gamma^{-1}|W_3|\,|\psi'(\boldsymbol{\rho}, \theta_n) + S(\boldsymbol{\rho})|W_m|e^{j\theta_m} - T(\boldsymbol{\rho})[N + |W_n|e^{j\theta_n}]|. \quad (27)$$

According to Theorem 1, a necessary and sufficient condition for (26) can be constructed as follows:

$$x_p(\boldsymbol{\rho}, \theta_m, \theta_n) < \Re\{\psi'(\boldsymbol{\rho}, \theta_n) + S(\boldsymbol{\rho})|W_m|e^{j\theta_m}\} \quad \forall\omega \in \Omega, \forall\{\theta_m, \theta_n\} \in [0, 2\pi]. \quad (28)$$

By gridding in ω, θ_m, and θ_n, then (28) becomes a convex constraint (with respect to $\boldsymbol{\rho}$); however, gridding in all of these variables can be computationally expensive. Therefore, a sufficient condition for (26) can be devised as follows:

$$\sup_{\omega\in\Omega} \frac{|W_3|[|\psi(\boldsymbol{\rho}) - NT(\boldsymbol{\rho})| + |C(\boldsymbol{\rho})W_n| + |S(\boldsymbol{\rho})W_m|]}{|\psi(\boldsymbol{\rho})| - |R(\boldsymbol{\rho})W_n| - |S(\boldsymbol{\rho})W_m|} < \gamma. \quad (29)$$

With this condition, the dependence in θ_m and θ_n has been removed, and gridding in only one variable (i.e., ω) is required.

The condition in (29) can be represented as a disk in the complex plane which is centered at $\psi(\boldsymbol{\rho})$ and has radius

$$x_r(\boldsymbol{\rho}) = \gamma^{-1}|W_3|[|\psi(\boldsymbol{\rho}) - NT(\boldsymbol{\rho})| + |C(\boldsymbol{\rho})W_n| + |S(\boldsymbol{\rho})W_m|] + |R(\boldsymbol{\rho})W_n| + |S(\boldsymbol{\rho})W_m|. \quad (30)$$

Therefore, a set of convex constraints is devised with $x_r(\boldsymbol{\rho}) < \Re\{\psi(\boldsymbol{\rho})\}$ for all $\omega \in \Omega$. This constraint has the same structure as that of the sensitivity functions and so can readily be included in the optimization problem. Note that (29) introduces some conservatism; however, this conservatism can always be reduced by imposing (28) (at the cost of a larger computation time).

Remark 1: For stable plants, $M = 1$ may be selected. Therefore, the disk uncertainty associated with M is $|W_m| = 0$. From (27) and (28), it can be observed that with $|W_m| = 0$, the dependence on θ_m is removed, and no gridding in θ_m is required. The necessary and sufficient condition then becomes

$$x_p(\boldsymbol{\rho}, \theta_n) < \Re\{\psi'(\boldsymbol{\rho}, \theta_n)\} \quad \forall\omega \in \Omega,\ \forall\theta_n \in [0, 2\pi] \quad (31)$$

where $x_p(\boldsymbol{\rho}, \theta_n) = \gamma^{-1}|W_3|\big|\psi'(\boldsymbol{\rho}, \theta_n) - T(\boldsymbol{\rho})[N + |W_n|e^{j\theta_n}]\big|$.

C. Controller Stability

Computation of an unstable controller should generally be avoided [17]. For the RST structure, it is evident that if the polynomial $S(z^{-1}, \boldsymbol{\rho})$ possesses zeros outside the unit circle, then the open-loop system will become unstable. In order to avoid this impairment, it is required to impose a constraint such that the polynomial $S(z^{-1}, \boldsymbol{\rho})$ possesses zeros inside the unit circle. This rationalization leads to the following lemma.

Lemma 2: Suppose that $S(z^{-1}, \boldsymbol{\rho})$ is parameterized as in (6). Then a sufficient (convex) condition to ensure that the zeros of $S(z^{-1}, \boldsymbol{\rho})$ remain inside the unit circle is

$$\Re\{S(\boldsymbol{\rho})\} > 0; \quad \forall\omega \in \Omega. \quad (32)$$

Proof: First note that a strictly positive real transfer function (and its inverse) is stable. $\Re\{S(\boldsymbol{\rho})\} > 0$ implies that the Nyquist diagram of $S(\boldsymbol{\rho})$ will not encircle the origin. Therefore, $S^{-1}(\boldsymbol{\rho})$ will not encircle the origin, and $S(\boldsymbol{\rho})$ is stable. ■

D. Convex Optimization via Semidefinite Programming

Suppose that it is desired to obtain $\mathcal{H}_\infty$ performance for a sensitivity function (i.e., minimize γ in $\|W_q\mathcal{S}_q\|_\infty < \gamma$). Then according to the results in Theorem 2, one can formalize an optimization problem to obtain the admissible $R(\boldsymbol{\rho})$, $S(\boldsymbol{\rho})$, and/or $T(\boldsymbol{\rho})$ controllers as follows:

$$\begin{aligned} &\min_{\gamma,\boldsymbol{\rho}}\ \gamma \\ &\text{s.t.: } \gamma^{-1}|W_q\Delta_q(\boldsymbol{\rho})| < \Re\{\psi(\boldsymbol{\rho})\} \\ &\qquad \forall\omega \in \Omega; \quad q \in \mathcal{Q}. \end{aligned} \quad (33)$$

The optimization problem in (33) is convex for a fixed value of γ. The classical solution to this problem is to implement a bisection algorithm in order to obtain the global solution.

The problem in (33) is known as a semiinfinite programming problem since there are a finite number of optimization variables and an infinite number of constraints. To solve this problem, the optimization algorithm can be converted to a semidefinite programming (SDP) problem. A predefined frequency grid can be implemented in order to solve a finite number of constraints. This frequency grid can be predefined in a variety of manners (see [9], [19]).

It can be shown that by increasing the controller order, the optimal solution to (33) converges to the global optimal solution of the $\mathcal{H}_\infty$ problem.

Lemma 3: Suppose that the RST controller achieves the optimal $\mathcal{H}_\infty$ performance for the plant model $G = NM^{-1}$ such that

$$\gamma_o = \sup_\omega |W_q\Delta_q(\boldsymbol{\rho})\psi^{-1}(\boldsymbol{\rho})|, \quad \forall q \in \mathcal{Q}.$$

In addition, suppose that γ_n is the optimal solution of the convex optimization in (33) when $R(\boldsymbol{\rho})$, $S(\boldsymbol{\rho})$, and/or $T(\boldsymbol{\rho})$ are parameterized by an nth order FIR filter. Then γ_n converges monotonically from above to γ_o when $n \to \infty$.

Proof: The proof of a similar condition has been established in [13] (for $q = 1$ and for a one-degree-of-freedom controller), and has been omitted to conserve space. However, the

TABLE I

PROCEDURE FOR COMPUTING AN RST CONTROLLER

Algorithm: Convex optimization for optimal performance
1. Excite the system with a multi-sinus or PRBS signal and identify the FRF of the system. If the process is stable, select $N = G$ and $M = 1$. If the process is unstable, see Section II-A for obtaining the coprime factors.
2. Compute the uncertainty for W_n and W_m using the covariance of the estimates [15] and define the performance filters in $\|W_q \mathcal{S}_q\|_\infty$.
3. Formulate the control problem as minimizing the infinity norm of multiple weighted sensitivity functions.
4. Start with a first-order RST controller and solve the optimization problem in (33) by using a frequency grid to obtain γ_n. The constraint should be modified based on which sensitivity function is considered.
5. If the desired performance is met, stop. Otherwise, increase the order by one (i.e., $n = n + 1$).
6. Solve the problem in (33) to obtain the new γ_n and go to Step 5.

necessary and sufficient condition from Theorem 2 can be combined with the ideas presented in [13] to ensure that the solution to (33) converges to the global optimal solution of the $\mathcal{H}_\infty$ problem as n increases ($\forall q \in \mathcal{Q}$). ■

Table I displays a general method for designing a controller using the proposed approach.

IV. CASE STUDIES

A. Case 1: Multi-Model Uncertainty

Consider the following unstable system reported in [20] which describes the dynamics of a magnetic levitation system linearized around an operating point (airgap of 17 mm):

$$G(s) = \frac{Y(s)}{U(s)} = \frac{\alpha_1}{(s + 131.3)(s - \alpha_2)(s + \alpha_2)} \tag{34}$$

where $\alpha_1 = 163863.6$ and $\alpha_2 = 29.85$. The input u is proportional to the inductor current and the output y is proportional the measured airgap. To demonstrate the effectiveness of the proposed method, it is supposed that there exists some uncertainty with the mass of the steel ball where the gain and poles of the system belong in the sets $\hat{\alpha}_1 \in \{0.9\alpha_1, \alpha_1, 1.1\alpha_1\}$ and $\hat{\alpha}_2 \in \{0.7\alpha_2, \alpha_2, 1.3\alpha_2\}$. With the proposed approach, a multimodel design can be implemented where stability and performance is guaranteed for all of the uncertainties associated with the system. The plant can be expressed as $G_l(s)$ for $l = 1, \ldots, 9$ (which represents the plant model with respect to the lth unique combination of the uncertain parameters).

Remark 2: Note that these models are simply used to obtain the FRFs of the plants and the controller synthesis does not rely on these parametric models. As a result, both continuous- and discrete-time plant models can be considered for the synthesis.

1) Performance Specifications: For this particular case study, it was desired to obtain the best performance for disturbance rejection (i.e., by minimizing $\|W_1 \mathcal{S}_1^l\|_\infty \ \forall l$ where $\mathcal{S}_1^l$ denotes the sensitivity function with respect to the lth plant model from the set G_l). Note that this is a regulation problem, and the polynomial $T(\boldsymbol{\rho})$ is not included in the design process. In addition, in order to have a zero steady-state error, the controller should include an integrator [i.e., $S(\boldsymbol{\rho}) = (1 - z^{-1})S'(\boldsymbol{\rho})$]. The weighting filter was selected as $W_1(s) = (s + \omega_d)s^{-1}$, which was designed in accordance with the methods described in [16]. The rejection bandwidth ω_d [rad s^{-1}] was selected as $\omega_d = 100\pi$. Note that $W_1(j\omega)$ is unbounded at $\omega = 0$; however, due to the fixed integrator in the controller, $\|W_1 \mathcal{S}_1^l\|_\infty$ remains bounded $\forall l$ and $\forall \omega$.

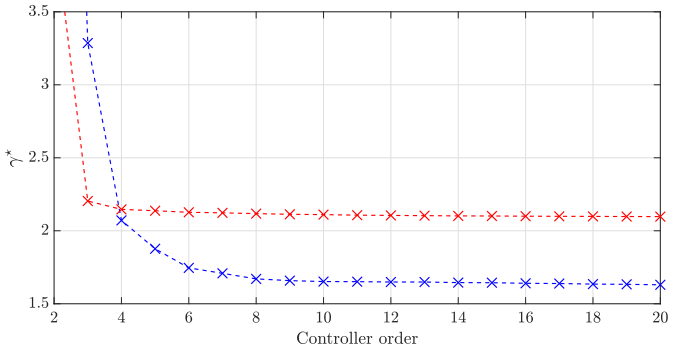

Fig. 3. Optimal solution $\gamma^\star$ as a function of the controller order. Solutions obtained with the proposed method (dashed-blue line); solutions obtained with the method from [21] (dashed-red line).

2) Controller Synthesis: Since each model is unstable, then each coprime factor must be selected such that $\{N_l(s), M_l(s)\} \in \mathscr{P}$ for all l. A simple choice is to divide both the numerator and denominator of each model by a factor $(s + 10)^3$.

Remark 3: If a parameteric model is not available for acquiring the FRFs of these coprimes, then a closed-loop identification experiment can be performed to obtain them (see Section II).

The problem in (33) was solved for $q = 1$ by considering all models in the set G_l and a linearly-spaced grid of 300 points from 0 to π/T_s rad s^{-1} (where a working sampling time of $T_s = 0.002$ s was selected, as asserted in [20]). The optimal solution $\gamma^\star$ for various controller orders have been computed and compared with the solutions obtained with the frequency-domain method in [21] (which requires the selection of a desired open-loop transfer function). Fig. 3 depicts the optimal solution as a function of the controller order; it can be observed that as the controller order increases, the solution obtained with the proposed method achieves better performance (i.e., converges monotonically to the global optimal solution of the $\mathcal{H}_\infty$ problem). For comparative purposes, the optimization times with both the proposed method and the method in [21] for a fifth-order controller (with $\gamma_{\max} = 5$, $\gamma_{\min} = 10^{-3}$, and a tolerance of 10^{-5} set for the bisection algorithm) are 111.5 s and 9.8 s, respectively. The difference in optimization times stems from the fact that the method in [21] fixes the polynomial $S(\boldsymbol{\rho})$ *a priori* such that $R(\boldsymbol{\rho})$ is the only polynomial to be optimized; with the proposed method, the parameters in both $R(\boldsymbol{\rho})$ and $S(\boldsymbol{\rho})$ are optimized. The optimization times were calculated based on a computer having the following hardware specifications: Intel-Core i7, 3.4 GHz CPU, and 8 GB RAM. The optimization algorithm was run using MATLAB version (R2015b) on a Windows 7 platform (64-b).

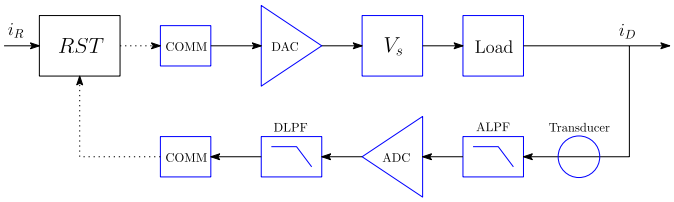

Fig. 4. Power converter control system.

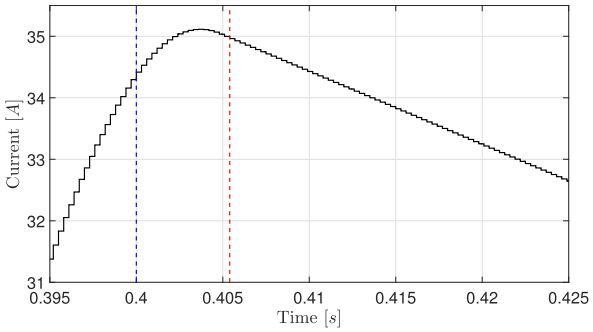

Fig. 5. Desired reference current profile. The blue-dashed line indicates the time when the error must remain within ±1000 parts-per-million (ppm); the dashed red line indicates the time when the error must remain within ±100 ppm.

B. Case 2: Power Converter Control

The general configuration of the CERN power converter control system is depicted in Fig. 4. The control loop consists of a magnet (i.e., the load), a voltage source V_s, low-pass antialiasing analog, and digital filters, a digital-to-analog converter (DAC), and an analog-to-digital converter (ADC). The DAC (optional) and ADCs are integrated in the control unit labeled as the function generator controller (FGC, [22]) whose main function is to execute the control algorithm. The main objective is to design an RST controller such that the error obtained from a specific desired current profile, shown in Fig. 5, meets the desired specifications.

The magnet is represented as an RL circuit, and the dynamics of this circuit are dominant over the other components of the system. Thus a first-order model with delay [i.e., $G_m(s) = e^{-sT_d}(L_m s + R_m)^{-1}$, where R_m is the circuit resistance, L_m is the circuit inductance, and T_d is the time delay] is appropriate to approximate the dynamics of the plant. For this case study, the model parameters are identified as: $R_m = 164.3$ mΩ, $L_m = 736.4$ μH, and $T_d = 275.4$ μs.

At CERN, the above model is discretized using the zero-order-hold method and used to design an RST controller based on the model-reference control (MRC) strategy [17]. The main difficulty is that the choice of the observer poles that lead to a good robustness margin is not trivial; the design of a working controller is a time-consuming iterative process.

A PRBS signal was used as the input voltage reference of the open-loop system in order to capture the dynamics of the process. A total of five experiments were performed with the PRBS clock period $T_{cl} = 100$ μs; the acquired periods (with transients removed in postprocessing) could then be merged together. A custom FGC signal is limited to 1023 samples; therefore, a 9-b PRBS signal was used for identification purposes. For a signal of length 511, the frequency resolution

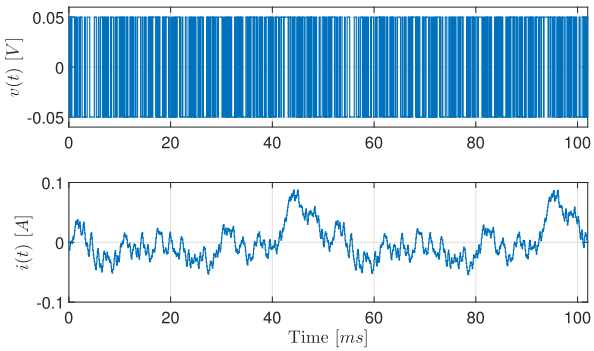

Fig. 6. PRBS signal used for the input voltage $v(t)$ of the open-loop system along with the resulting output current $i(t)$.

is limited to 255 points. The uncertainty was obtained from the covariance of the estimates with a 95% confidence interval. Fig. 6 shows the input and output signals acquired from the identification experiment.

1) Weighting Filter Selection: For this particular case study, it was desired to obtain the best tracking performance (i.e., by minimizing $\|W_3\mathcal{S}_3\|_\infty$) while ensuring reasonable stability margins. It is evident that $\mathcal{S}_2^d + \mathcal{S}_3^d = 1$, where $\mathcal{S}_2^d$ and $\mathcal{S}_3^d$ are the desired complementary and error sensitivity functions, respectively. Based on this condition, the weighting filter W_3 was selected as $W_3 = [\mathcal{S}_3^d]^{-1}$. $\mathcal{S}_2^d$ was chosen as a standard second-order model $\mathcal{S}_2^d(s) = \omega_d^2(s^2+2\zeta\omega_d s+\omega_d^2)^{-1}$, where ζ is the damping factor and

$$\omega_d = 2\pi f_d\left[1 - 2\zeta^2 + \sqrt{2 - 4\zeta^2 + 4\zeta^4}\right]^{-0.5}$$

and f_d [Hz] is the desired closed-loop bandwidth.

A simulation was performed to determine the required bandwidth to satisfy the desired error specifications. At CERN, the error is calculated with respect to a delayed reference input (i.e., $e(t) = r(t-\tau) - y(t)$); τ is determined by shifting the reference signal such that the minimum peak error is achieved. By assuming that the closed-loop response behaves as $\mathcal{S}_2^d$, the bandwidth f_d can be selected such that the error between the delayed reference input and output remains within the requirements set by the application (which are shown in Fig. 5); the simulation results led to $f_d = 300$ Hz and $\zeta = 0.8$.

2) Synthesis and Experimental Results: The voltage applied to the magnet by the voltage source and the relative current are both sampled at 10 kHz while the control loop is run 3 times slower (i.e., $T_s = 300$ μs). Since the plant is stable, then a possible selection for the coprime factors is $N(e^{-j\omega}) = G(e^{-j\omega})$ and $M(e^{-j\omega}) = 1$. With a minimum value of $m_d = 0.5$ set for the modulus margin [i.e., the minimum distance between the critical point $(-1+j0)$ and the Nyquist plot of the open-loop transfer function], the following optimization problem must be solved:

$$\begin{aligned} &\min_{\gamma,\boldsymbol{\rho}} \ \gamma \\ &\text{s.t.: } \Re\{\psi(e^{-j\omega_k},\boldsymbol{\rho})\} > x_r(e^{-j\omega_k},\boldsymbol{\rho}) \\ &\qquad \Re\{\psi(e^{-j\omega_k},\boldsymbol{\rho})\} > x_m(e^{-j\omega_k},\boldsymbol{\rho}) \\ &\qquad \Re\{S'(e^{-j\omega_k},\boldsymbol{\rho})\} > 0 \end{aligned} \tag{35}$$

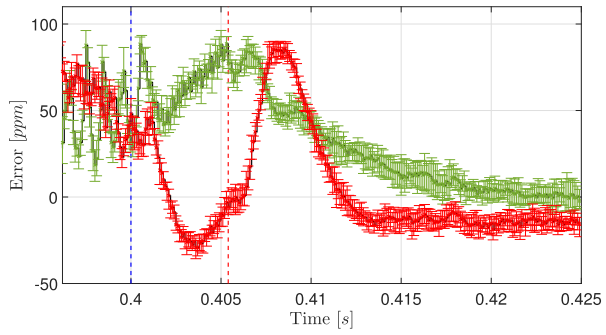

Fig. 7. Comparison between the error resulting from the model-based design (solid-black line with red error-bars) and the error resulting with the proposed method (solid-black line with green error-bars).

for $k = 1, \ldots, 255$, where $S(z^{-1}, \boldsymbol{\rho}) = (1 - z^{-1})^2\, S'(z^{-1}, \boldsymbol{\rho})$, $x_r(e^{-j\omega_k}, \boldsymbol{\rho})$ is defined as in (30), and $x_m(e^{-j\omega_k}, \boldsymbol{\rho}) = |m_d S(e^{-j\omega_k}, \boldsymbol{\rho})| + |R(e^{-j\omega_k}, \boldsymbol{\rho}) W_n(e^{-j\omega_k})|$. The first inequality in (35) ensures that $\mathcal{H}_\infty$ nominal performance is achieved for the RST structure whilst considering the frequency dependent uncertainties. The second inequality ensures that the modulus margin is at least 0.5 (a requirement for robust stability at CERN). The third inequality ensures that $S(\boldsymbol{\rho})$ has no unstable zeros (another requirement at CERN).

The SDP solver (SDPT3) was used in conjunction with MATLAB to perform the bisection algorithm [23]. A ninth-order controller was used to achieve the desired results (by following the steps outlined in Section III-D). An optimal value of $\gamma^\star = 1.202$ was obtained after 61.3 s using the same computer as in the previous example.

A total of ten experiments were performed; the error for both the model-based MRC method and data-driven-based designs (with the associated error bars showing the minimum and maximum errors at each sampling instant) is shown in Fig. 7. It can be observed that both designs are comfortably within the ± 1000 ppm fast-transient requirement and within the ± 100 ppm steady-state requirement. Indeed, both controllers achieve ± 100 ppm even during the fast transients. However, the proposed method ensures that all of the design requirements are met while eliminating the iterative process of attaining robust performance from the model-based methodology.

V. Conclusion

The necessary and sufficient conditions for the existence of RST controllers that achieve $\mathcal{H}_\infty$ performance for multiple weighted sensitivity functions have been established with a set of convex constraints. In addition, constraints have been devised in order to design a controller which considers the frequency-dependent uncertainties and to assure the controller stability. The simulation and experimental results show that the proposed data-driven method offers an optimization-based systematic approach that leads to low-order RST controllers meeting the challenging specifications required by each application. For future work, the extension of the method to multivariable systems will be investigated.

References

[1] Z.-S. Hou and Z. Wang, "From model-based control to data-driven control: Survey, classification and perspective," *Inf. Sci.*, vol. 235, pp. 3–35, Jun. 2013.

[2] A. S. Bazanella, L. Campestrini, and D. Eckhard, *Data-Driven Controller Design: The H_2 Approach*. Dordrecht, The Netherlands: Springer, 2012.

[3] R. Hoogendijk, A. J. den Hamer, G. Angelis, R. van de Molengraft, and M. Steinbuch, "Frequency response data based optimal control using the data based symmetric root locus," in *Proc. IEEE Int. Conf. Control Appl.*, Yokohama, Japan, Sep. 2010, pp. 257–262.

[4] S. Khadraoui, H. Nounou, M. Nounou, A. Datta, and S. P. Bhattacharyya, "Robust control design method for uncertain system using a set of measurements," in *Proc. Amer. Control Conf. (ACC)*, 2013, pp. 4325–4330.

[5] S. Khadraoui, H. Nounou, M. Nounou, A. Datta, and S. P. Bhattacharyya, "A control design method for unknown systems using frequency domain data," in *Proc. 9th Asian Control Conf. (ASCC)*, 2013, pp. 1–6.

[6] A. J. den Hamer, S. Weiland, and M. Steinbuch, "Model-free norm-based fixed structure controller synthesis," in *Proc. 48th IEEE Conf. Decision Control*, Shanghai, China, Dec. 2009, pp. 4030–4035.

[7] A. Karimi and G. Galdos, "Fixed-order H_∞ controller design for nonparametric models by convex optimization," *Automatica*, vol. 46, no. 8, pp. 1388–1394, 2010.

[8] A. Karimi and Z. Emedi, "H_∞ gain-scheduled controller design for rejection of time-varying narrow-band disturbances applied to a benchmark problem," *Eur. J. Control*, vol. 19, no. 4, pp. 279–288, 2013.

[9] G. Galdos, A. Karimi, and R. Longchamp, "H_∞ controller design for spectral MIMO models by convex optimization," *J. Process Control*, vol. 20, no. 10, pp. 1175–1182, 2010.

[10] M. Saeki, M. Ogawa, and N. Wada, "Low-order H_∞ controller design on the frequency domain by partial optimization," *Int. J. Robust Nonlinear Control*, vol. 20, no. 3, pp. 323–333, 2010.

[11] M. Hast, K. J. Åström, B. Bernhardsson, and S. Boyd, "PID design by convex-concave optimization," in *Proc. Eur. Control Conf.*, Zurich, Switzerland, 2013, pp. 4460–4465.

[12] S. Boyd, M. Hast, and K. J. Åström, "MIMO PID tuning via iterated LMI restriction," *Int. J. Robust Nonlinear Control*, vol. 26, no. 8, pp. 1718–1731, 2016.

[13] A. Karimi, A. Nicoletti, and Y. Zhu, "Robust H_∞ controller design using frequency-domain data via convex optimization," *Int. J. Robust Nonlinear Control*, Jul. 2016, doi: 10.1002/rnc.3594.

[14] A. Nicoletti, Z. Emedi, and A. Karimi, "A data-driven approach in designing RST controllers with H_∞ performance via convex optimization," in *Proc. 54th IEEE Conf. Decision Control (CDC)*, Osaka, Japan, Dec. 2015, pp. 6650–6655.

[15] L. Ljung, *System Identification: Theory for the User*, 2nd ed. Englewood Cliffs, NJ, USA: Prentice-Hall, 1999.

[16] K. Zhou and J. C. Doyle, *Essentials of Robust Control*. Englewood Cliffs, NJ, USA: Prentice-Hall, 1998.

[17] I. D. Landau and G. Zito, *Digital Control Systems: Design, Identification and Implementation*. London, U.K.: Springer-Verlag, 2006.

[18] A. Rantzer and A. Megretski, "A convex parameterization of robustly stabilizing controllers," *IEEE Trans. Autom. Control*, vol. 39, no. 9, pp. 1802–1808, Sep. 1994.

[19] P. Seiler, B. Vanek, J. Bokor, and G. J. Balas, "Robust H_∞ filter design using frequency gridding," in *Proc. Amer. Control Conf. (ACC)*, 2011, pp. 1801–1806.

[20] J. Salt, A. Sala, and P. Albertos, "A transfer-function approach to dual-rate controller design for unstable and non-minimum-phase plants," *IEEE Trans. Control Syst. Technol.*, vol. 19, no. 5, pp. 1186–1194, Sep. 2011.

[21] G. Galdos, A. Karimi, and R. Longchamp, "RST controller design by convex optimization using frequency-domain data," in *Proc. 18th IFAC World Congr.*, Milan, Italy, 2011, pp. 11429–11434.

[22] D. Calcoen, Q. King, and P. F. Semanaz, "Evolution of the CERN power converter function generator/controller for operation in fast cycling accelerators," in *Proc. Int. Conf. Accel. Large Experim. Control Syst. (ICALEPCS)*, Grenoble, France, 2011, pp. 939–942.

[23] K. C. Toh, M. J. Todd, and R. H. Tütüncü, "SDPT3—A MATLAB software package for semidefinite programming, version 1.3," *Optim. Methods Softw.*, vol. 11, nos. 1–4, pp. 545–581, 1999.